

COMPUTATIONAL FLUID DYNAMICS IN SUPPORT OF THE SNS LIQUID MERCURY THERMAL-HYDRAULIC ANALYSIS^a

Mark W. Wendel
Oak Ridge National Laboratory^b
P. O. Box 2008, MS-6415
Oak Ridge, TN, 37831
(423)574-2825

Graydon L. Yoder
Oak Ridge National Laboratory^b
P. O. Box 2008, MS-8045
Oak Ridge, TN, 37831
(423)574-5282

Moshe Siman-Tov
Oak Ridge National Laboratory^b
P. O. Box 2008, MS-8045
Oak Ridge, TN, 37831
(423)574-6515

ABSTRACT

Experimental and computational thermal-hydraulic research is underway to support the liquid mercury target design for the Spallation Neutron Source (SNS) facility. The SNS target will be subjected to internal nuclear heat generation that results from pulsed proton beam collisions with the mercury nuclei. Recirculation and stagnation zones within the target are of particular concern because of the likelihood that they will result in local hot spots and diminished heat removal from the target structure. Computational fluid dynamics (CFD) models are being used as a part of this research. Recent improvements to the 3D target model include the addition of the flow adapter which joins the inlet/outlet coolant pipes to the target body and an updated heat load distribution at the new baseline proton beam power level of 2 MW. Two thermal-hydraulic experiments are planned to validate the CFD model.

I. INTRODUCTION

The Spallation Neutron Source (SNS) will have a 2-MW pulsed proton beam with a pulse duration of 0.5Fs, pulse frequency of 60 Hz, and elliptical beam cross section of 7×20 cm. This beam will impinge on a liquid mercury target contained within a stainless steel vessel. About 60% of the beam power is deposited in the mercury target.¹ Figure 1 shows a schematic for the target body design. In addition to thermal shock and materials compatibility, key feasibility issues for the target are related to its thermal-hydraulic performance.

Because the liquid mercury is in a steady flow condition during operation of the SNS, it does not require an additional cooling system as would be necessary for a solid target. However, the mercury must also serve as the coolant for the stainless steel target containment vessel. It is necessary to ensure that the temperatures and thermal gradients remain acceptably low, especially in the stainless steel containment. The target pressure drop must also be considered because it directly affects structural loading and required pumping power.

The proton beam is parallel to the predominant direction of flow. The portion of the stainless steel containment which is impacted by the beam is called the target window. The highest heat loads are located in this window, so a supplemental exterior (mercury) coolant flow is provided by a jacket that wraps around the target lengthwise. This will be referred to as the window coolant flow channel. The main part of the flow, which is separated from this window coolant flow has a much more complex flow pattern with the two inlet streams turning 90° around the flow baffles, impacting one another, then joining into a single return channel. Flow separation occurs at the baffles, and the combined return flow reattaches to the back side of both baffles.

Computational fluid dynamics (CFD) is being used to assess the thermal-hydraulic performance of the SNS target by providing flow visualization and quantifying critical parameters. The simplest approach to the fluid dynamics analysis is to time-average the problem. This averaging is

^aThe submitted manuscript has been authored by a contractor of the U.S. Government No. DE-AC05-96OR22464. Accordingly, the U.S. Government retains a nonexclusive, royalty-free license to publish or reproduce the published form of this contribution, or allow others to do so, for U.S. Government purposes.

^bOak Ridge National Laboratory is managed by the Lockheed Martin Energy Research Corp. for the U.S. Department of Energy under Contract No. DE-AC05-96OR22464.

accomplished by spreading the pulse energy evenly throughout the entire pulse period of 0.01667s, thus allowing the simulation to be performed as a steady state. An additional level of averaging is assumed in order to apply the Reynolds-averaged two-equation turbulence model. The steady-state solution should provide a reasonable estimate for the overall flow pattern and temperature distribution within the target enclosure. Also of concern, however, are transient effects which occur on the microsecond time scale and which impact the target performance. These effects include small spatial and temporal variations in the flow field and pressure waves induced by rapid thermal expansion (density decrease) of the heated liquid. This CFD model is useful for looking at compressibility effects such as these transient pressure waves. However, the fluid/structure interaction at the wall, which is crucial, cannot be represented without additional code development.

The model from which the present results were produced uses a 2-MW-beam heat generation profile based on an updated understanding of the neutron transport within the target. The model is a full three-dimensional (3-D) representation of the liquid mercury and stainless steel in the target body (Fig. 2). Also, a long transition piece that joins the target body to the inlet/outlet pipes has been added. The stainless steel structure of the transition piece is not included in the model since the heat load is negligible. Previous CFD analyses^{2,3} were performed for a 1 MW beam, with half of the current target flow rate, and without the transition piece included.

CFD support has also been provided to the experiments that are planned for assessing the feasibility of the target design. One of these experiments, the Mercury Thermal-Hydraulic Loop (MTHL), will be used to measure heat transfer coefficients to liquid mercury in a long thin channel, directly applicable to the window flow channel geometry. Another experiment, the Water Thermal Hydraulic Loop (WTHL), will be used for full scale target flow visualization and measurements. This experiment will be used to directly validate the CFD model. CFD analysis has been used to design the MTHL test section for uniform flow distribution and minimal pressure losses. A model has also been used to scale the WTHL such that the water flows will yield results relevant to the mercury flow in the actual target.

II. DESCRIPTION OF MODEL

The general-purpose CFD code CFX4.2,⁴ which uses a finite-volume, pressure-correction method, is being used to compute the temperature and velocity distribution in the liquid-mercury/stainless-steel target. The model includes solid conducting regions that represent the stainless steel target walls and internal baffle. Heat generation is modeled

in both of these regions. A renormalization-group (RNG) isotropic, two-equation turbulence model provided by CFX is used in combination with the standard law-of-the-wall boundary condition for imposing wall heat fluxes in the energy equation and shear stress in the momentum equations.

The boundary conditions include no-slip at the walls (simulated by turbulence wall functions), specified velocity at the inlets, and specified pressure at the outlet boundaries. The density is assumed to be constant, but the viscosity and thermal conductivity are allowed to vary with temperature.

Only one-half of the target is modeled, assuming bilateral symmetry. Computational and experimental investigations into the adequacy of this symmetry assumption have shown that it does not strictly hold due to a flow instability. However, near the target window, where the highest heat loads exist, the symmetry assumption is good. Asymmetry occurs only downstream in the return duct. Although the main flow through the target has an additional (horizontal) geometric plane of symmetry, the cooling-jacket flow is not symmetric about this plane since it flows from the bottom to the top.

The discretization used for the CFD model of the target with transition piece includes 1.4 million computational cells. Without the transition piece, only 0.7 million cells are used. Computational cell dimensions vary from 0.001 m near the tip of the flow baffle up to 0.100 m in the streamwise direction at the end of the model furthest from the window. The grid was carefully selected to keep transitions in grid size smooth and to place the near wall nodes at a distance from the wall that would satisfy the requirement of the turbulent law-of-the-wall condition. This requirement is that the node next to the wall must be located outside of the laminar sublayer ($30 < y^+ < 200$).

Liquid mercury enters the window cooling channel from seven subchannels (three and one-half of which are modeled due to symmetry) located on the bottom of the target, then returns to another seven subchannels on the top of the target. At the nose, all of the window-coolant mercury flows together in a common plenum region that gradually narrows in thickness from 3mm down to 1 mm at the horizontal midplane (Fig. 3). All of the subchannel details and channel geometry were closely approximated.

The assumptions include an inlet temperature of 353 K and a total target heat loading of 1.2 MW, corresponding to the 2-MW proton beam (60% of the energy is deposited in the target). An elliptic beam cross section is assumed with a parabolic power distribution, as shown for the horizontal midplane in Fig. 4. The mass flow rate is assumed to be 293

kg/s, corresponding to an average velocity of 1.43 m/s in the two inlet channels of the main target body.

Steady-state convergence from a zero initial condition required a few weeks of CPU time on a 466 MHz DEC ALPHAserver 4100. A level of convergence was obtained such that the cumulative mass conservation error was less than 0.3% of the total target mass flow rate.

III. COMPUTATIONAL RESULTS

Two simulations were performed: one with the transition piece, and one without. Speed contours on four slices through the computational domain are shown in Fig. 5 for the case with the transition piece. The computed speed contours for both cases on the horizontal midplane are shown in Fig. 6. The results are very different when the piping transition piece is included. Both simulations (with and without the transition piece) show a large recirculation zone downstream of the flow baffle around which the liquid mercury makes the U-turn. This large zone obstructs about one-half of the cross-sectional area in the central rectangular channel. Results are very different, however, in the inlet channel of the main target body. The abrupt area change formed by the transition piece and the main target body at the inlet produces a jet which separates from the wall and generates a lot of turbulent energy in the “shadow” of the area change (Fig. 7). Without the transition piece, an additional small recirculation zone was predicted on the centerline near the window where the heat load is the highest. However, the greater turbulent energy in the simulation with the transition piece leads to higher eddy diffusivity (proportional to the square of turbulent kinetic energy) and the elimination of this recirculation pattern.

A closeup of the results with the transition piece reveals flow details near the front window and within the window cooling channel (Fig. 8). Here it can be seen that no separation from the wall is predicted in this region. Speed in the window coolant channel, which is the same for both cases, can also be seen in this figure.

A comparison of the temperature distribution with and without the transition piece is shown in Fig. 9. A $k-\epsilon$, RNG turbulence model was employed for these two simulations. This model uses a turbulent Prandtl number (0.9 was assumed here) to scale the thermal diffusivity with the eddy diffusivity based on Reynolds analogy. The elevated turbulence intensity when the transition piece is modeled leads to the elimination of the hot spot in the main flow due to increased thermal diffusion. The peak temperature, which is predicted on the outer wall of the window cooling jacket, is 27EC lower than the results without the transition piece. Since the large recirculation zone on the back side of the

flow baffle lay directly in the proton beam path where the heat is deposited, a secondary maximum occurs in the temperature distribution at this location. A comparison for the two cases of the predicted maximum temperatures is shown in Table 1.

The total irreversible pressure loss in the main flow where the transition piece is not included is 9 kPa, most of which is due to the separating flow around the baffle. With the transition piece represented, the predicted loss is a much higher 60 kPa, due to the abrupt expansion at the inlet.

Table 1. Predicted peak temperatures for CFX simulations of SNS target.

	Without Transition Piece	With Transition Piece
Peak mercury temperature near window	198EC	138EC
Peak mercury temperature in recirculation zone	144EC	147EC
Peak stainless steel temperature	191EC	171EC

IV. CONCLUSIONS

The predicted thermal-hydraulic performance of the SNS target for 2-MW operation with a parabolic beam profile has been presented based on 3-D CFD calculations. The assumed thermal limit of the target due to material-strength considerations is 200EC. The predicted target temperatures are acceptably low (peak temperature of 173EC). The abrupt expansion that occurs between the inlet transition piece and the inlet channels in the main target body is very beneficial to cooling of the target. This sudden expansion (1.8 area ratio) produces turbulent kinetic energy that results in improved thermal mixing (turbulent diffusion) inside the window at the front of the target, reducing the peak temperature in the structure by 20EC. However this improved thermal result comes at a cost to the target pressure drop, which is 6.5 times higher than without the area change.

Due to concern regarding the accuracy of the turbulence model, parametric investigations of the sensitivity of the results to the selection of turbulence model, inlet turbulence,

and turbulent Prandtl number are currently underway. Also, experimentally obtained values will be available from the WTHL for turbulence intensity for comparison to the CFD results.

Because of the large variations in speed within the beam path, the peak temperatures are strongly dependent on beam power distribution. Therefore, parametric studies are also planned that investigate the sensitivity of the peak temperatures and temperature gradients to beam alignment and characterization. Future data from a full-scale water experiment and a separate effect experiment for heat transfer to liquid mercury will be used to validate the computational model.

REFERENCES

1. J. R. Haines et al., "Overview of the Target Systems for the Spallation Neutron Source," *AccApp '98*, Gatlinburg, TN, September 20–23, 1998.

2. M. W. Wendel, M. Siman-Tov, "CFD Analysis of a Liquid Mercury Target for the National Spallation Neutron Source," *Proc. ASME Fluids Engineering Division Summer Mtg.*, June 22–26, 1997.

3. M. W. Wendel, M. Siman-Tov, "Three-Dimensional Computational Fluid Dynamics for the Spallation Neutron Source Liquid Mercury Target," *AccApp '98*, Gatlinburg, TN, September 20–23, 1998.

4. *CFX-4.2: SOLVER*, User's Manual, AEA Technology, CFX International, Oxfordshire, United Kingdom, December 1997.

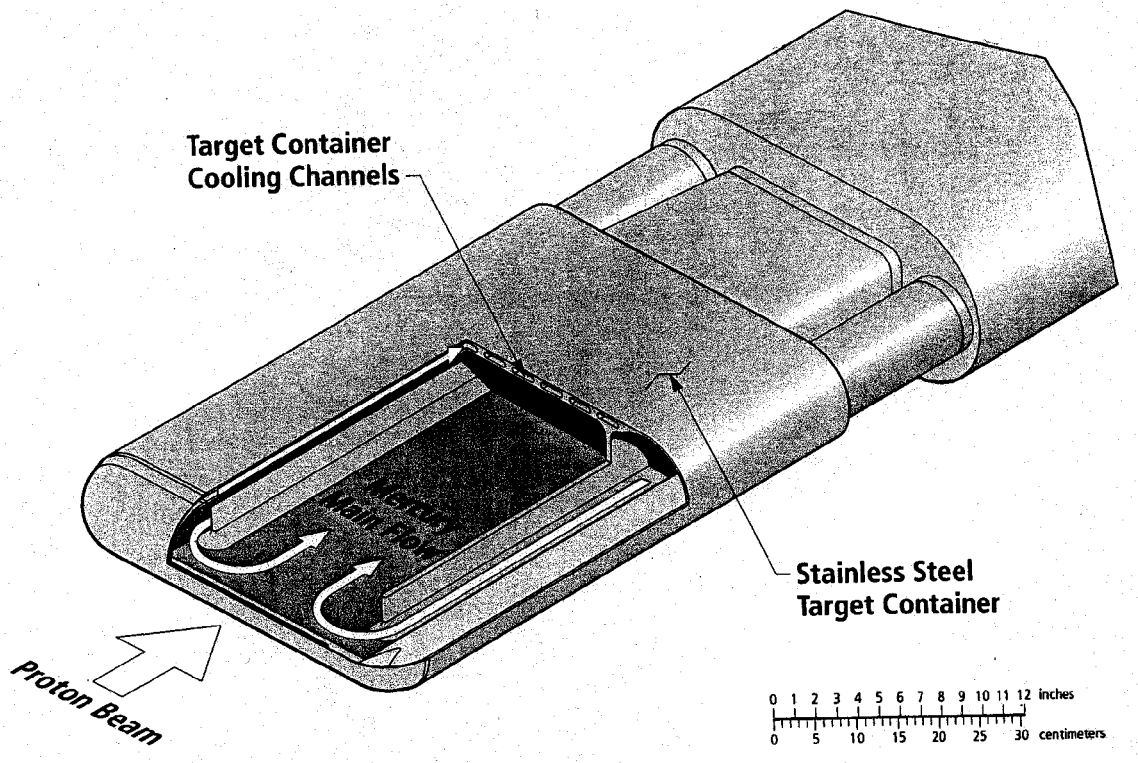


Fig. 1. Diagram of SNS target design.

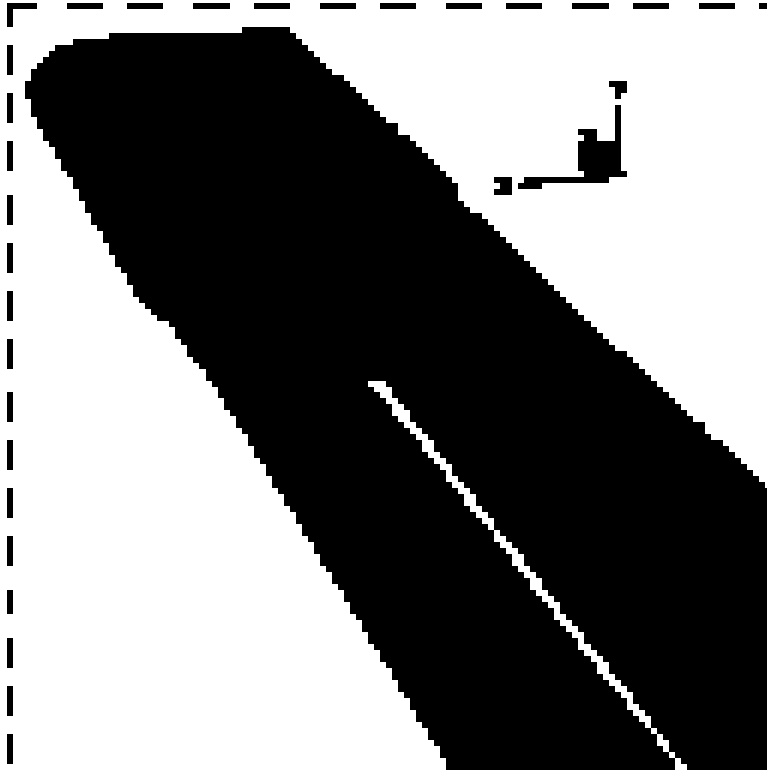


Fig. 2. Rear view of computational domain, which assumes bilateral symmetry, including the piping inlet/outlet transition pieces.

File Contains Data for PostScript Printers Only

Fig. 3. Window coolant channel geometry. Only stainless steel is shown (one half of the target has been removed).



Fig. 4. Heat generation on horizontal midplane.

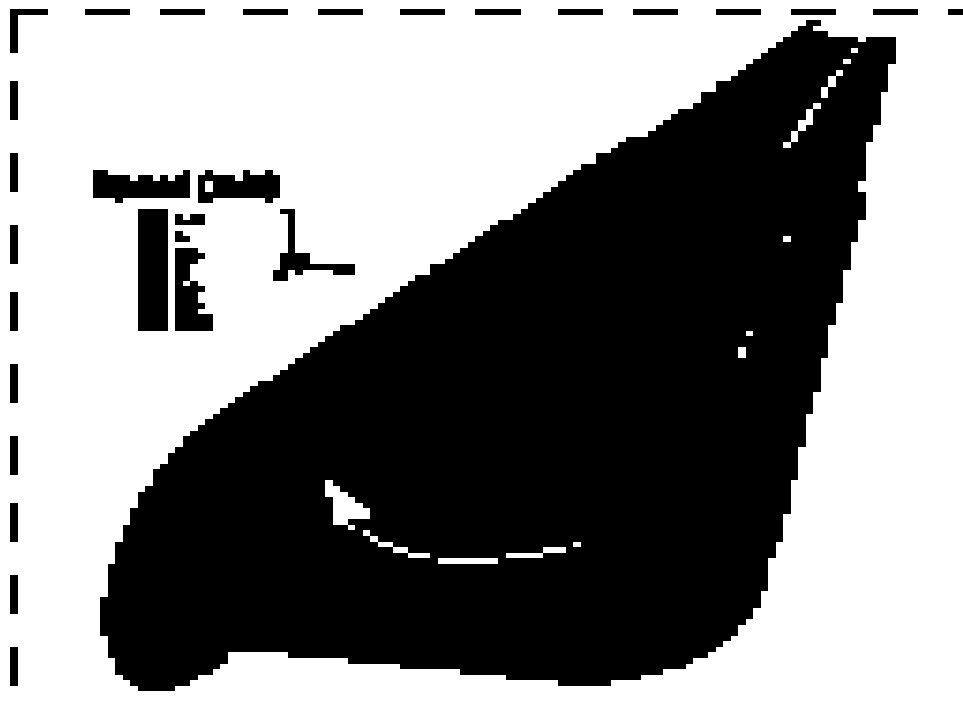


Fig. 5. Computed flow field (speed) on four slices through the computational domain.

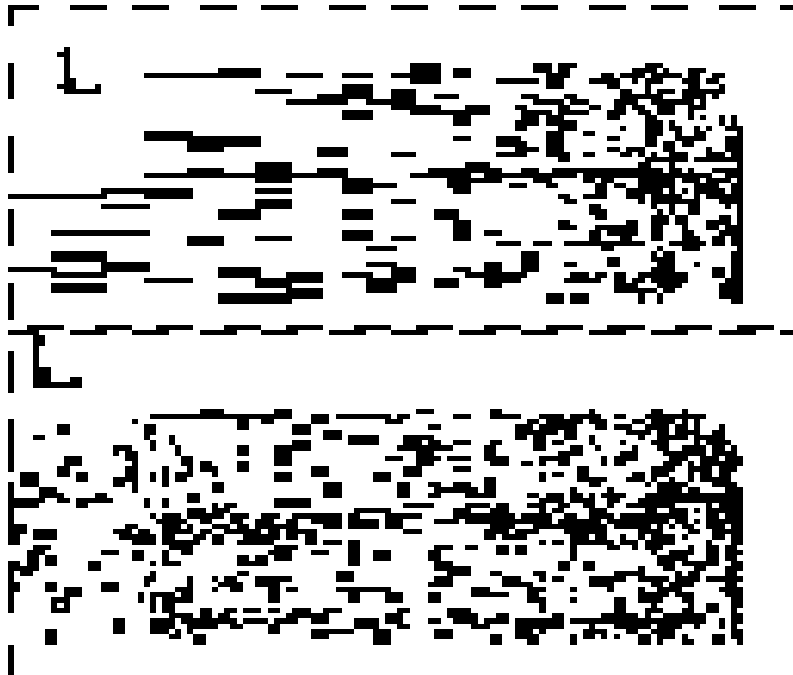


Fig 6. Comparison of speed distribution on horizontal midplane for analysis without (top) and with (bottom) the transition piece.

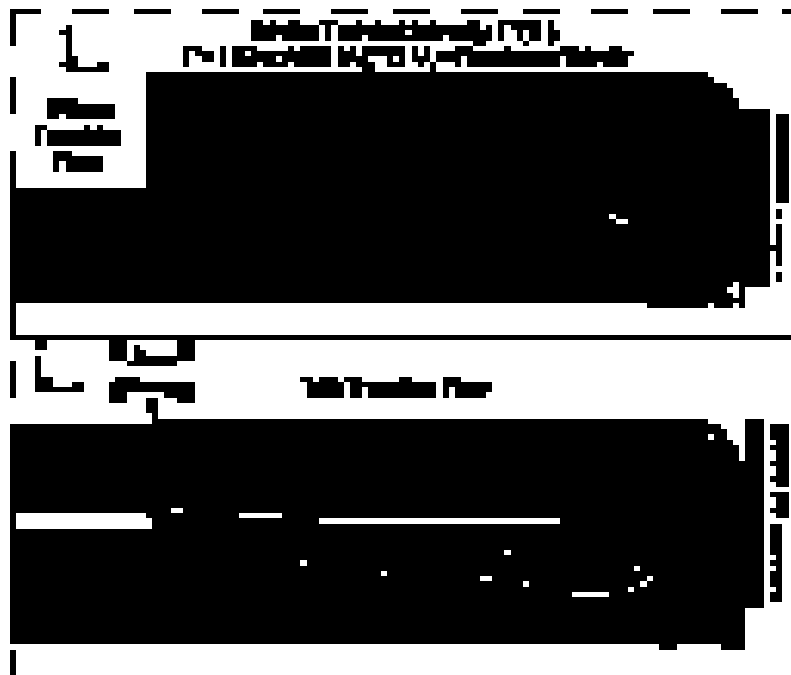


Fig. 7. Turbulent intensity computed on the horizontal midplane for two simulations.

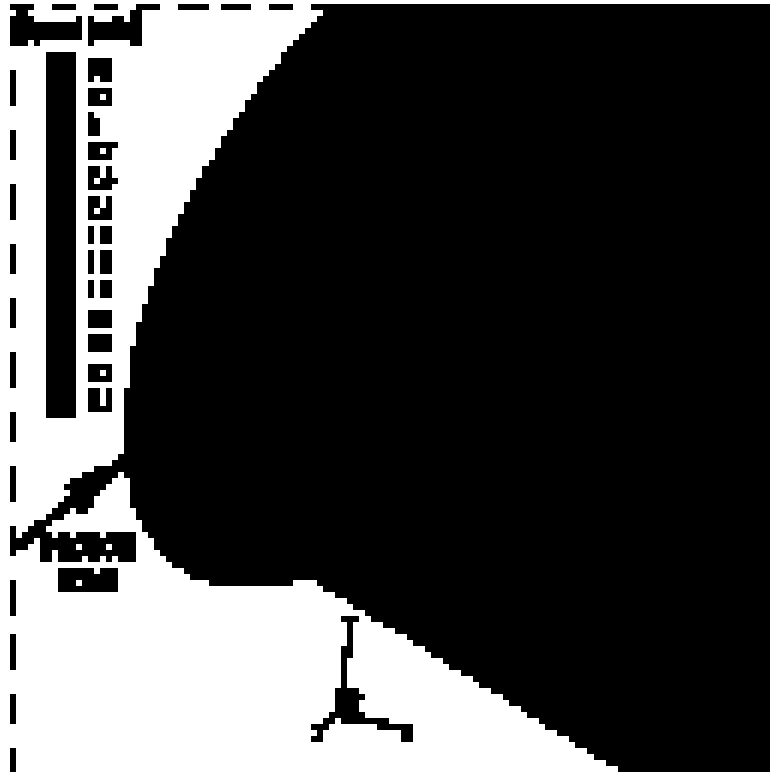


Fig. 8. Close-up near the front window of the target showing speed and streamlines.



Fig. 9. Comparisons of peak temperatures near front window for analysis with and without the transition piece.